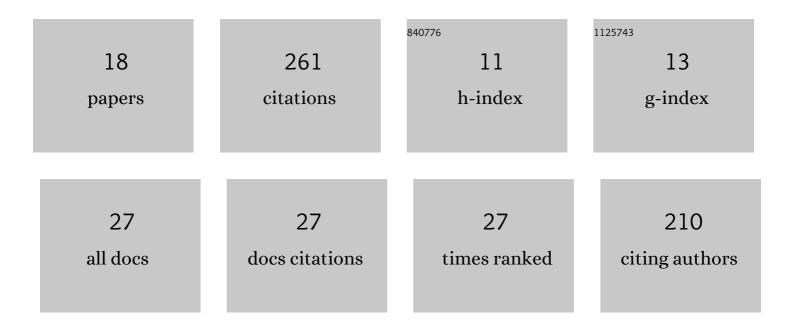
Takeshi Akuhara

List of Publications by Year in descending order

Source: https://exaly.com/author-pdf/5329401/publications.pdf Version: 2024-02-01



#	Article	IF	CITATIONS
1	Marine Sediment Characterized by Oceanâ€Bottom Fiberâ€Optic Seismology. Geophysical Research Letters, 2020, 47, e2020GL088360.	4.0	53
2	Hydrous state of the subducting Philippine Sea plate inferred from receiver function image using onshore and offshore data. Journal of Geophysical Research: Solid Earth, 2015, 120, 8461-8477.	3.4	35
3	Segmentation of the Vp/Vs ratio and lowâ€frequency earthquake distribution around the fault boundary of the Tonankai and Nankai earthquakes. Geophysical Research Letters, 2013, 40, 1306-1310.	4.0	22
4	Overpressured Underthrust Sediment in the Nankai Trough Forearc Inferred From Transdimensional Inversion of Highâ€Frequency Teleseismic Waveforms. Geophysical Research Letters, 2020, 47, e2020GL088280.	4.0	21
5	Performance of Seismic Observation by Distributed Acoustic Sensing Technology Using a Seafloor Cable Off Sanriku, Japan. Frontiers in Marine Science, 2022, 9, .	2.5	21
6	Application of cluster analysis based on waveform cross-correlation coefficients to data recorded by ocean-bottom seismometers: results from off the Kii Peninsula. Earth, Planets and Space, 2014, 66, .	2.5	15
7	Sedimentary Structure Derived From Multiâ€Mode Ambient Noise Tomography With Dense OBS Network at the Japan Trench. Journal of Geophysical Research: Solid Earth, 2021, 126, e2021JB021789.	3.4	15
8	Subsurface Imaging With Oceanâ€Bottom Distributed Acoustic Sensing and Water Phases Reverberations. Geophysical Research Letters, 2022, 49, .	4.0	15
9	A fluidâ€rich layer along the Nankai trough megathrust fault off the Kii Peninsula inferred from receiver function inversion. Journal of Geophysical Research: Solid Earth, 2017, 122, 6524-6537.	3.4	13
10	Non-linear waveform analysis for water-layer response and its application to high-frequency receiver function analysis using OBS array. Geophysical Journal International, 2016, 206, 1914-1920.	2.4	12
11	Beyond Receiver Functions: Green's Function Estimation by Transdimensional Inversion and Its Application to OBS Data. Journal of Geophysical Research: Solid Earth, 2019, 124, 1944-1961.	3.4	12
12	Distributed Acoustic Sensing measurement by using seafloor optical fiber cable system off Sanriku for seismic observation. , 2019, , .		11
13	Receiver Function Imaging of the Amphibious NE Japan Subduction Zone—Effects of Lowâ€Velocity Sediment Layer. Journal of Geophysical Research: Solid Earth, 2021, 126, e2021JB021918.	3.4	9
14	Lithosphere–asthenosphere boundary beneath the Sea of Japan from transdimensional inversion of S-receiver functions. Earth, Planets and Space, 2021, 73, .	2.5	7
15	Segmentation of Hypocenters and 3-D Vp/Vs Ratio Structure around the Kii Peninsula Revealed by Onshore and Offshore Seismic Observations. , 2013, , .		0
16	A Fluid-Rich Layer Along the Megathrust Fault Inferred from High-Frequency Receiver Function Inversion Analysis. Springer Theses, 2018, , 65-82.	0.1	0
17	Receiver Function Image of the Subducting Philippine Sea Plate. Springer Theses, 2018, , 43-64.	0.1	0
18	Precise aftershock distribution of the 2019 Yamagata-oki earthquake using newly developed simple anchored-buoy ocean bottom seismometers and land seismic stations. Earth, Planets and Space, 2022, 74, .	2.5	0